



Alzheimer's Disease Early Diagnosis Based on Resting-State Dynamic Functional Connectivity

Fei Xie*

Electronic and Information
Engineering College, Tongji
University, Shanghai, China
xief@tongji.edu.cn

Xiaoliang Gong[†]

Electronic and Information
Engineering College, Tongji
University, Shanghai, China
gxllshsh@tongji.edu.cn

Tongqi Wu

Software College, Tongji University,
Shanghai, China
1750701@tongji.edu.cn

Zhenghao He

Electronic and Information
Engineering College, Tongji
University, Shanghai, China
2954383503@qq.com

Yan Lu

Electronic and Information
Engineering College, Tongji
University, Shanghai, China
robinluaa@outlook.com

Mohan Zhao

Electronic and Information
Engineering College, Tongji
University, Shanghai, China
1951854@tongji.edu.cn

ABSTRACT

Functional magnetic resonance imaging (fMRI) technology has been widely used in the diagnosis of Alzheimer's disease, but there are some problems such as high data dimension and unclear characteristics. The nonlinear complex network of different brain regions based on the Lyapunov exponents and approximate entropy are extracted in this work. The open data set ADNI (Alzheimer's disease neuroimaging initiative) are used to test. The results show that in the other three different groups and patients with Alzheimer's disease, the accuracy of the classification results using SVM (support vector machine) classifier at the whole brain voxel level can reach more than 99%, which is better than the classification results using the correlation of the original time series. Our findings provide new insights into the complexity of brain structural networks in the process of Alzheimer's disease and other mental diseases.

CCS CONCEPTS

• **Applied computing** → Life and medical sciences; Computational biology; Biological networks.

KEYWORDS

Lyapunov Exponent, Approximate Entropy, Nonlinear Complex Network

ACM Reference Format:

Fei Xie, Xiaoliang Gong, Tongqi Wu, Zhenghao He, Yan Lu, and Mohan Zhao. 2023. Alzheimer's Disease Early Diagnosis Based on Resting-State

* [Author Introduction] Fei Xie, Master student. Research interest: Brain MRI imaging process, E-mail: xief@tongji.edu.cn

[†] [Corresponding author] Xiaoliang Gong, Ph.D., engineer, Research interest: Brain and Cognitive Intelligent computing research and teaching, E-mail: gxllshsh@tongji.edu.cn

Permission to make digital or hard copies of all or part of this work for personal or classroom use is granted without fee provided that copies are not made or distributed for profit or commercial advantage and that copies bear this notice and the full citation on the first page. Copyrights for components of this work owned by others than the author(s) must be honored. Abstracting with credit is permitted. To copy otherwise, or republish, to post on servers or to redistribute to lists, requires prior specific permission and/or a fee. Request permissions from permissions@acm.org.

ICSCA 2023, February 23–25, 2023, Kuantan, Malaysia

© 2023 Copyright held by the owner/author(s). Publication rights licensed to ACM.

ACM ISBN 978-1-4503-9858-9/23/02...\$15.00

<https://doi.org/10.1145/3587828.3587881>

Dynamic Functional Connectivity. In *2023 12th International Conference on Software and Computer Applications (ICSCA 2023), February 23–25, 2023, Kuantan, Malaysia*. ACM, New York, NY, USA, 6 pages. <https://doi.org/10.1145/3587828.3587881>

1 INTRODUCTION

Alzheimer's disease is an uncontrollable neurological brain disease. Therefore, early intervention and treatment are essential. Effectively distinguishing different populations is helpful to study the biomarkers of disease development, for better intervention and treatment of patients. Studies have found that the information flow between different brain regions can distinguish people with different degrees of disease [1]. In terms of the structure and function of the brain, the human brain is one of the most complex information processing systems, and some characteristics of nonlinearity can be used in studies to characterize the functional connectivity properties between brain regions [2].

Based on complex network theory, the analysis of nonlinear properties of time series has been evolving. The Lyapunov exponent based on chaos theory can detect the degree of chaos in the system, the approximate entropy is a non-negative value to represent the complexity of the time series. Measurement of Lyapunov exponent and entropy has been widely used in the diagnosis of mental disease. Research showed significant lower values for the largest Lyapunov exponent for patients with metabolic encephalopathy compared to normal [3]. Ghahfarrokhi used nonlinear complexity indicators-Lyapunov exponent and approximate entropy to diagnose human brain tumors with an accuracy of 82.5% [4].

In this study, the dynamic complexity analysis method of nonlinear characteristic Lyapunov exponent and approximate entropy is applied to the classification and diagnosis of Alzheimer's disease in different courses, and the brain area correlation network is constructed by global analysis of the brain. Finally, SVM, RF (random forest) and AdaBoost cross validation are used for classification research to assist the diagnosis of AD and provide a new perspective for the early diagnosis of AD.

Table 1: Demographic and clinical information of the participants.

Group	NC	EMCI	LMCI	AD
Age(years)	75.77 ± 5.2	72.41 ± 6.1	74.29 ± 7.21	75.41 ± 6.20
Sex(M/F)	11/20	16/22	20/11	14/16

2 MATERIALS AND DATA PREPROCESSING

2.1 Participants

The data set used in this study is from ADNI (Alzheimer’s disease neuroimaging initiative) database, an integrated longitudinal multi-center study to develop clinical, imaging, genetic, and biochemical biomarkers (<https://adni.loni.usc.edu/>) [5]. All subjects were scanned in a three-tesla (3T) scanner with 140 functional volumes. All the data was scanned in the resting state, which is the state of being awake with your eyes closed. According to the type of disease, there are a total of 31 NC(normal control), 38 EMCI (early mild cognitive impairment) patients, 31 LMCI (late mild cognitive impairment) patients and 30 AD patients. Detailed demographic and clinical information are shown in Table 1.

Data collection parameters are set as follows: field strength =3.0 T; manufacturer = Philips Medical Systems; slice thickness = 3.3 mm; repetition time (TR) = 3000 ms; echo time (TE) = 30 ms; and slice number = 48.

2.2 Data Preprocessing

DPABI toolbox based on MATLAB platform was used to preprocess the data in batches [6], the first 10 time points were removed to avoid signal interference due to the instability of the initial moment. Then time layer correction, head movement correction, space standardization and smoothing were operated successively. Time layer correction can synchronize the acquisition time series of different subjects. Head movement correction can reduce the impact of head movement on data quality to a certain extent. In the pre-processing, the subjects with head movement translation > 2mm or rotation movement > 2° were removed. For spatial standardization, in order to minimize the interference error caused by individual differences, the brain images of each subject were registered to the MNI305 standard spatial template invented by Montreal Neurological Institute in Canada [7]. In spatial smoothing, a Gaussian kernel with full width at half maximum (FWHM) of 6 mm is used to improve the signal-to-noise ratio and reduce the mismatches between individuals [8]. Since the signal noise of human brain is large and there are many uncertain factors, all the signals were averaged to filter the noise, so as to obtain a more stable signal.

3 METHODS

3.1 Lyapunov Exponent

It is possible to visualize whether a system or mapping is a chaotic system through the Lyapunov exponent image mapping [9]. Lyapunov exponent represents the numerical characteristics of the average exponential divergence rate of adjacent trajectories in phase space [10]. Lyapunov exponent is usually used to judge the chaos of the system. Through the image, we can intuitively see whether the system or mapping is chaotic or non-chaotic. The logistic mapping

of Lyapunov exponent is:

$$x_{n+1} = ax_n (1 - x_n)$$

the calculation formula of Lyapunov exponent is:

$$\lambda = \lim_{n \rightarrow \infty} \sum_{k=0}^{n-1} \log \left| \frac{df}{dx} \right|_{x_k}, \left| \frac{df}{dx} \right|_{x_k} = a - 2ax_k$$

where x is the time series and a is the value range of the mapping.

3.2 Approximate Entropy

Approximate entropy is used to describe the irregularity of the system [11]. It is a random complexity, which can reflect the difference between the probability of mutual approximation of the patterns of broken line segments connected by m adjacent points and the probability of mutual approximation of the patterns of broken line segments connected by $m + 1$ points. The expression of the correlation coefficient is as follows:

Firstly, taking m as the window size, n time series are divided into $k = n - m + 1$ series,

$$y_i(t) = (x_i(t), x_{i+1}(t), \dots, x_{i+m-1}(t))$$

Then calculate the Euclidean distance $d\{y(i), y(j)\}$ between any component of $y(i)$ and $y(j)$, and define the maximum distance between each component as the maximum contribution component distance $D\{y(i), y(j)\}$, as shown below:

$$D\{y(i), y(j)\} = \max\{|y(i+k) - x(j+k)|\}$$

where $i, j = 1, 2, \dots, n - m + 1, k = 0, 1, \dots, m - 1$.

Define a threshold T , and the ratio of the number greater than T to the total number $n - m + 1$ in each row of the statistics table is denoted as $C_i^m(t)$, according to k $C_i^m(t)$, take the logarithmic average as:

$$\Phi^m(t) = \frac{1}{n - m + 1} \sum_{i=1}^{n-m+1} \ln C_i^m(t)$$

where $T = r * SD$, r is a coefficient between 0.1 and 0.25, and SD is the time series’ standard deviation.

Finally, increase the window length to $m + 1$ and repeat the previous steps, the approximate entropy can be calculated as:

$$ApEn(t) = \Phi^m(t) - \Phi^{m+1}(t)$$

3.3 Pearson’s Correlation Coefficient

When exploring the relationship between variables in the data as a whole, we want to know how one variable will change when another changes. The index reflecting this relationship is called the correlation coefficient [12], and the expression formula of the correlation coefficient is as follows:

$$r(X, Y) = \frac{\text{Cov}(X, Y)}{\sqrt{\text{Var}(X) \text{Var}(Y)}}$$

where $Cov(X, Y)$ is the covariance between X and Y , $Var(X)$ is the variance of X , and $Var(Y)$ is the variance of Y .

Generally, the following points need to be paid attention to for the correlation coefficient: the range of correlation coefficient r is -1 to 1 ; the greater the absolute value of r , the stronger the correlation; the positive and negative of r represents the direction of correlation, positive values represent positive correlation, and negative values represent negative correlation.

3.4 Machine Learning Classifier

SVM is a kind of pattern recognition method based on statistical theory. It can solve the problem of nonlinear data classification well by mapping the linear non-fractional data into the high-dimensional linear feature space with kernel function, and then performing linear classification [13]. SVM classifier is selected because it can find the optimal classification surface of data, is not so sensitive to the number of features, and is suitable for high-dimensional and small-sample data. In this study, we used polynomial kernel function with power of 2.

RF algorithm is a bagging ensemble algorithm, which generally selects the decision tree as a weak classifier. It combines multiple weak classifiers, and finally determines the final classification result through the voting results or the number of base learners [14]. The model has high accuracy, generalization performance and strong anti over fitting ability. Besides, cross validation was used to evaluate the effect of the model. In this study, we used a random forest model with 50 subtrees for classification. Besides, the performance is evaluated by cross validation. For each classification test, we used 5-fold cross validation and repeated it 20 times.

AdaBoost algorithm is an adaptive enhanced iterative integration algorithm [15]. Its main principle is to train multiple weak classifiers on the same training set, and finally, the results of all classifiers are weighted and combined to get the final classification result. The algorithm used in this study is the improved algorithm of AdaBoost. For the classification results of the previous classifier, the weight of the samples with wrong classification results remains unchanged, and the weight of the samples with correct classification is reduced to train the next weak classifier. In this study, the parameter of the classifier is set as: cycle index=1000, learning rate = 0.05.

4 RESULTS

In this section, the classification results of the two classifier models based on the complex matrix are presented. We also visualize the complexity correlation matrices for time series, Lyapunov exponent and approximate entropy. The models' input drawn by using three indicators of 90 ROI brain regions is shown in Figures 1-3.

In Figures 1 and 3, the functional connectivity of the whole brain ROI and Approximate entropy is significantly lower in AD patients, but the difference between the other three groups is not significant. In Figure 2, the decrease in functional connectivity of Lyapunov exponent is more pronounced in the other three groups compared to normal individuals. Overall, various patients have abnormal ROI and nonlinear functional connectivity, so we use machine learning classifiers to explore the classification effects of those features.

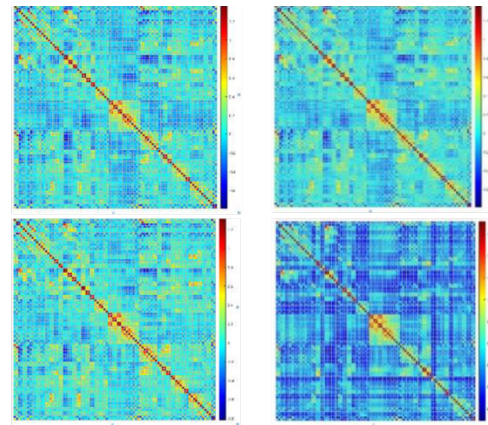


Figure 1: The correlation matrix drawn by using time singals (the first row from left to right is NC, EMCI, the second row from left to right is LMCI and AD)

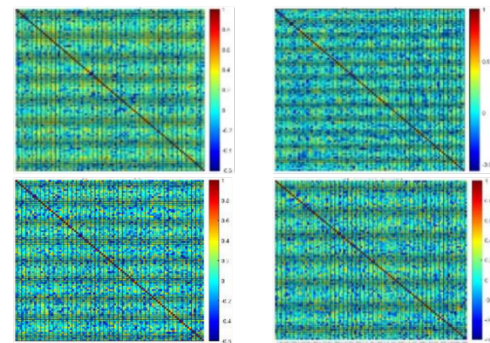


Figure 2: The correlation matrix drawn by using Approximate entropy (the first row from left to right is NC, EMCI, the second row from left to right is LMCI and AD)

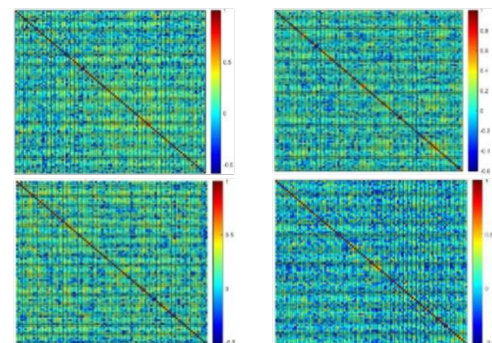


Figure 3: The correlation matrix drawn by using Lyapunov exponent (the first row from left to right is NC, EMCI, the second row from left to right is LMCI and AD)

Table 2: The classification results of the SVM algorithm in the four groups.

ACC (mean \pm SD) %SEN (mean \pm SD) %SPE (mean \pm SD) %	Complex network		
	RSFC	Nonlinear	
		AEFC	LEFC
NC&EMCI	76.25 \pm 7.01	96.94 \pm 3.33	96.53 \pm 4.72
	75.56 \pm 6.54	94.44 \pm 6.42	96.11 \pm 6.95
NC&LMCI	76.94 \pm 9.92	99.44 \pm 1.76	97.78 \pm 2.87
	80.16 \pm 5.03	96.94 \pm 1.58	96.67 \pm 2.87
	81.72 \pm 4.38	97.22 \pm 2.93	98.33 \pm 2.68
NC&AD	80.69 \pm 2.57	96.67 \pm 3.88	95.00 \pm 6.65
	99.47 \pm 1.16	96.82 \pm 3.18	96.67 \pm 3.15
	98.94 \pm 2.33	97.78 \pm 2.87	94.44 \pm 5.86
EMCI&LMCI	100.00 \pm 0.00	95.56 \pm 4.38	98.89 \pm 2.34
	83.47 \pm 5.66	92.78 \pm 4.76	95.00 \pm 4.68
	81.11 \pm 5.10	99.44 \pm 1.76	99.44 \pm 1.76
EMCI&AD	85.83 \pm 8.35	86.11 \pm 9.53	90.56 \pm 9.82
	99.53 \pm 1.05	94.72 \pm 2.05	97.78 \pm 1.76
	99.06 \pm 2.10	95.00 \pm 4.86	96.67 \pm 2.87
LMCI&AD	100.00 \pm 0.00	94.44 \pm 2.62	98.89 \pm 2.34
	99.22 \pm 1.48	97.22 \pm 2.55	96.67 \pm 2.87
	98.44 \pm 2.96	96.11 \pm 3.75	94.44 \pm 5.86
	100.00 \pm 0.00	96.00 \pm 3.93	98.89 \pm 2.34

ACC: accuracy; SEN: sensitivity; SPE: specificity; SD: standard deviation

RSFC: resting-state functional connectivity; AEFC: Approximate entropy functional connectivity; LEFC: Lyapunov exponent functional connectivity

4.1 Support Vector Machine Classification Results

We calculate the correlation values in the whole brain region by using the original signals and two nonlinear complex indicators. Table 2 shows the pairwise classification results of the SVM algorithm in the four groups of people. The better of the three types of feature classification results in the table is bolded.

4.2 Random Forest Classification Results

Table 3 shows the pairwise classification results of the random forest algorithm in the four groups of people.

4.3 AdaBoost Classification Results

Table 4 shows the pairwise classification results of the AdaBoost algorithm in the four groups of people.

5 DISCUSSION

In this section, we conduct study and analysis for the discriminative effect of the three indicators. The representation and analysis of the output complexity of the human brain system can indicate the health and stability of its mental state [16].

5.1 Three Indicators

Machine learning classifiers were used to demonstrate that the mutual information amount and entropy correlation of the four groups are significantly different. The same classifier parameter setting was applied to classify the correlation matrix. As can be seen

in tables 2 and 3, the classification accuracy using ROI correlation is higher in the comparison with AD patients, but in the other three groups, the classification effect of nonlinear feature correlation is more significant. Table 4 shows that nonlinear correlation achieved relatively good results in all six groups of comparisons. In addition, the three tables also show the better classification performance of SVM on small sample and high-dimensional data.

This result verifies nonlinear complex attribute of the brain. The complexity of a brain's topological network changes during the course of the disease, as the severity of the disease increases, the complexity of the system decreases [17]. It is more consistent with the state of the system to reflect the network complexity by using the circulation of nonlinear characteristics between different brain regions [18]. It can better characterize the damage of the brain system network [19], which provides a new idea for the early diagnosis of disease.

5.2 Comparison

In the end, the best classification results of the complexity characteristics of nonlinear networks are used to compare with the research results presented in the article. Besides, the same classifier used in previous study is also used in our research. Table 5 shows the results of this paper compared with previous studies, and the better results of this paper are bolded. Our result of more than 99% accuracy was comparable to those in previous researches.

Table 3: The classification results of the random forest algorithm in the four groups.

ACC (mean ± SD) %SEN (mean ± SD) %SPE (mean ± SD) %	Complex network		
	RSFC	Nonlinear	
		AEFC	LEFC
NC&EMCI	56.11±7.29	66.67±7.54	64.31±5.50
	53.89±4.30	63.33±5.26	60.83±4.92
	58.33±5.98	70.00±6.87	67.78±9.81
NC&LMCI	57.78±7.19	66.94±8.73	68.19±7.18
	57.22±6.94	65.83±14.56	65.00±3.26
	58.33±3.62	68.06±9.34	71.39±9.58
NC&AD	99.17±1.31	73.47±6.53	70.56±8.80
	99.44±1.71	74.44±9.77	68.89±3.17
	98.89±2.28	72.50±11.61	72.22±7.66
EMCI&LMCI	53.06±7.51	73.47±9.12	63.89±7.04
	55.28±5.99	75.00±6.81	66.67±6.09
	50.83±7.56	71.94±7.30	61.11±9.87
EMCI&AD	98.89±1.40	69.31±7.24	77.92±5.73
	98.61±2.47	71.11±9.90	78.33±7.84
	99.17±2.04	67.50±8.00	77.50±9.79
LMCI&AD	98.06±1.82	79.58±5.58	72.08±5.94
	98.33±2.61	76.67±9.97	69.44±10.43
	97.78±3.32	82.50±9.24	74.72±11.61

Table 4: The classification results of the AdaBoost algorithm in the four groups.

ACC (mean ± SD) %SEN (mean ± SD) %SPE (mean ± SD) %	Complex network		
	RSFC	Nonlinear	
		AEFC	LEFC
NC&EMCI	68.21±4.52	75.56±7.29	69.03±8.22
	68.75±9.66	72.78±5.62	67.78±10.45
	71.83±7.33	78.33±8.70	70.28±7.22
NC&LMCI	69.58±6.59	76.94 ± 1.58	73.89±6.40
	70.56±13.38	77.22 ± 2.93	78.89±7.98
	68.61±15.74	76.67 ± 3.88	68.89±10.24
NC&AD	72.50±5.52	80.97±6.58	80.28±6.68
	60.00±5.04	76.94±9.06	74.72±8.29
	89.05±0.00	85.00±7.21	85.83±9.79
EMCI&LMCI	70.42±5.12	66.39±5.29	73.19±9.83
	68.06±7.83	73.89±9.55	81.67±8.08
	72.78±8.44	78.89±9.47	84.72±9.74
EMCI&AD	77.50±5.52	84.58±7.05	80.69±7.73
	80.00±4.04	68.89±7.87	70.83±8.74
	75.00±4.43	90.28±6.29	90.56±9.53
LMCI&AD	79.86±5.02	81.53±6.06	86.25±5.21
	65.00±8.94	75.28±6.42	79.44±9.28
	94.72±2.33	87.78±8.34	83.06±9.45

6 CONCLUSION

In this paper, we extracted the nonlinear complex network of different brain regions based on the Lyapunov exponents and approximate entropy of functional magnetic resonance signals. These nonlinear complex networks are effective feature representations of lesions in patients with Alzheimer's disease, which are proved by

three typical machine learning classifiers: SVM, RF and AdaBoost. This study shows that brain complexity indicators change accordingly as the disease progresses, which provides a new idea for early diagnosis of the disease.

Table 5: Comparison with previous studies for the classification.

Groups	Others			Ours		
	Brain region	Feature	Acc (%)	Brain region	Feature(complex network)	Acc (%)
AD-LMCI	the whole brain [20]	RSFC	0.89	the whole brain	AEFC	0.96
EMCI-LMCI		RSFC	0.90		LEFC	0.95
		callosum	RSFC		0.46	
	fibers [21]					
AD-NC	DMN, SN and CEN	dFC	0.95		AEFC	0.96
AD-MCI	[22]		0.94		LEFC	0.97
NC-MCI			0.77		AEFC	0.96

RSFC: resting-state functional connectivity; dFC: dynamic functional connectivity

LEFC: Lyapunov exponent functional connectivity; AE: approximate entropy functional connectivity; SN: saliency network; CEN: central executive network

7 LIMITATIONS

The current study has some limitations. Changes in the complexity of local brain regions were not explored, and also the sample size was relatively small. Future studies could focus more on these two aspects to provide more insights.

REFERENCES

- Liang L, Yuan Y, Wei Y, Yu B, Mai W, Duan G, Nong X, Li C, Su J, Zhao L, Zhang Z and Deng D. 2021. Recurrent and concurrent patterns of regional BOLD dynamics and functional connectivity dynamics in cognitive decline. *J. Alzheimers Res Ther* 13,1 (Jan 2021), 28. <https://doi.org/10.1186/s13195-020-00764-6>
- Jose O. Maximo, Cailee M. Nelson and Rajesh K. Kana. 2021. "Unrest while Resting"? Brain entropy in autism spectrum disorder. *J. Brain Research* 1762 (Jul 2021), 147435. <https://doi.org/10.1016/j.brainres>
- Jacob JE, Cheria A, Gopakumar K, Iype T, Yohannan DG and Divya KP. Can Chaotic Analysis of Electroencephalogram Aid the Diagnosis of Encephalopathy? *J. Neurol Res Int* 2018 (May 2018), 8192820. <https://doi.org/10.1155/2018/8192820>
- Sepehr Salem Ghahfarrokhi and Hamed Khodadadi. 2020. Human brain tumor diagnosis using the combination of the complexity measures and texture features through magnetic resonance image. *J. Biomedical Signal Processing and Control* 61 (Aug 2020), 102025. <https://doi.org/10.1016/j.bspc.2020.102025>
- Jack, C.R., Jr., Bernstein, M.A., Fox, N.C., Thompson, P., Alexander, G., Harvey, D., Borowski, B., Britson, P.J., L. Whitwell, J., Ward, C., Dale, A.M., Felmlee, J.P., Gunter, J.L., Hill, D.L., Killiany, R., Schuff, N., Fox-Bosetti, S., Lin, C., Studholme, C., DeCarli, C.S., Gunnar Krueger, Ward, H.A., Metzger, G.J., Scott, K.T., Mallozzi, R., Blezek, D., Levy, J., Debbs, J.P., Fleisher, A.S., Albert, M., Green, R., Bartzokis, G., Glover, G., Mugler, J. and Weiner, M.W. 2008. The Alzheimer's disease neuroimaging initiative (ADNI): MRI methods. *J. Magn. Reson. Imaging* 27,4 (Apr 2008), 685-691. <https://doi.org/10.1002/jmri.21049>
- Chao-Gan Y and Yu-Feng Z. 2010. DPARSF: A MATLAB Toolbox for "Pipeline" Data Analysis of Resting-State fMRI. *J. Front Syst Neurosci* 4, 13 (May 2010). <https://doi.org/10.3389/fnsys.2010.00013>
- Tzourio-Mazoyer N, Landeau B, Papathanassiou D, Crivello F, Etard O, Delcroix N, Mazoyer B and Joliot M. 2002. Automated anatomical labeling of activations in SPM using a macroscopic anatomical parcellation of the MNI MRI single-subject brain. *J. Neuroimage* 15, 1(Jan 2002), 273-89. <https://doi.org/10.1006/nimg.2001.0978>
- Sokunbi MO, Cameron GG, Ahearn TS, Murray AD and Staff RT. 2015. Fuzzy approximate entropy analysis of resting state fMRI signal complexity across the adult life span. *J. Med Eng Phys* 37, 11 (Nov 2015), 1082-1090. <https://doi.org/10.1016/j.medengphy.2015.09.001>
- Wang Z, Lou H and Sun J. 2011. fMRI functional connectivity analysis of anxiety disease patients based on spatiotemporal Lyapunov exponent method. *J. Zhongguo Yi Liao Qi Xie Za Zhi* 35, 4 (Jul 2011), 294-7. Chinese.
- Keilholz S, Maltbie E, Zhang X, Yousefi B, Pan WJ, Xu N, Nezafati M, LaGrow TJ and Guo Y. 2020. Relationship Between Basic Properties of BOLD Fluctuations and Calculated Metrics of Complexity in the Human Connectome Project. *J. Front Neurosci* 15, 14(Sep 2020), 550923. <https://doi.org/10.3389/fnins.2020.550923>
- Li Lin and Fulei Chu. 2011. Approximate entropy as acoustic emission feature parametric data for crack detection. *J. Nondestructive Testing and Evaluation* 26, 02 (Jul 2011), 119-128. <https://doi.org/10.1080/10589759.2010.521825>
- Xiao L, Cai B, Qu G, Zhang G, Stephen JM, Wilson TW, Calhoun VD and Wang YP. 2022. Distance Correlation-Based Brain Functional Connectivity Estimation and Non-Convex Multi-Task Learning for Developmental fMRI Studies. *J. IEEE Trans Biomed Eng* 69, 10 (Oct 2022), 3039-3050. <https://doi.org/10.1109/TBME.2022.3160447>
- Qiong Liu, Qiong Gu and Zhao Wu. 2017. Feature selection method based on support vector machine and shape analysis for high-throughput medical data. *J. Computers in Biology and Medicine* 91,(Dec 2017) 103-111. <https://doi.org/10.1016/j.compbiomed.2017.10.008>
- Kamarajan C, Ardekani BA, Pandey AK, Kinreich S, Pandey G, Chorlian DB, Meyers JL, Zhang J, Bermudez E, Kuang W, Stimus AT and Porjesz B. 2022. Differentiating Individuals with and without Alcohol Use Disorder Using Resting-State fMRI Functional Connectivity of Reward Network, Neuropsychological Performance, and Impulsivity Measures. *J. Behav Sci (Basel)* 12, 5 (Apr 2022), 128. <https://doi.org/10.3390/bs12050128>
- Li, X and Li, K. 2022. High-dimensional imbalanced biomedical data classification based on P-AdaBoost-PAUC algorithm. *J Supercomput* 78, 14(Sep 2022), 16581-16604. <https://doi.org/10.1007/s11227-022-04509-0>
- Goldberger AL, Peng CK and Lipsitz LA. 2002. What is physiologic complexity and how does it change with aging and disease? *J. Neurobiology of Aging* 23, 1 (Jan-Feb 2002), 23-26. [https://doi.org/10.1016/s0197-4580\(01\)00266-4](https://doi.org/10.1016/s0197-4580(01)00266-4)
- John, M., Ikuta, T. and Ferbinteanu, J. 2017. Graph analysis of structural brain networks in Alzheimer's disease: beyond small world properties. *J. Brain Struct Funct* 222 (Dec 2020), 923-942. <https://doi.org/10.1007/s00429-016-1255-4>
- Abásolo D, Escudero J, Hornero R, Gómez C and Espino P. 2008. Approximate entropy and auto mutual information analysis of the electroencephalogram in Alzheimer's disease patients. *J. Med Biol Eng Comput* 46, 10(Oct 2008), 1019-28. <https://doi.org/10.1007/s11517-008-0392-1>
- Sun J, Wang B, Niu Y, Tan Y, Fan C, Zhang N, Xue J, Wei J and Xiang J. 2020. Complexity Analysis of EEG, MEG, and fMRI in Mild Cognitive Impairment and Alzheimer's Disease: A Review. *J. Entropy (Basel)* 22, 2(Feb 2020), 239. <https://doi.org/10.3390/e22020239>
- Bi Xia-an, Xu Qian, Luo Xianhao, Sun Qi and Wang Zhigang. 2018. Analysis of Progression Toward Alzheimer's Disease Based on Evolutionary Weighted Random Support Vector Machine Cluster. *J. FRONTIERS IN NEUROSCIENCE* 12 (Oct 2018), 1662-453X. <https://www.frontiersin.org/articles/10.3389/fnins.2018.00716>
- Jitsuishi, T and Yamaguchi, A. 2022. Searching for optimal machine learning model to classify mild cognitive impairment (MCI) subtypes using multimodal MRI data. *J. Sci Rep* 12,1 (Mar 2022), 4284. <https://doi.org/10.1038/s41598-022-08231-y>
- Meng X, Wu Y, Liang Y, Zhang D, Xu Z, Yang X and Meng L. 2022. A Triple-Network Dynamic Connection Study in Alzheimer's Disease. *J. Front Psychiatry* 13 (Apr 2022), 862958. <https://doi.org/10.3389/fpsy.2022.862958>